Terrestrial heat flow in Lake Superior[1]

S.R. HART
Woods Hole Oceanographic Institution, Woods Hole, MA 02543, U.S.A.

J.S. STEINHART
5000 Sequoia Road, Albuquerque, NM 87120, U.S.A.

AND

T.J. SMITH
Department of Mathematics, Kalamazoo College, Kalamazoo, MI 49007, U.S.A.

Received March 16, 1993
Revision accepted October 30, 1993

Using oceanographic heat-flow techniques, 162 measurements of heat flow were made in Lake Superior during the summers of 1966 and 1967. These data are of high quality, with precisions with respect to intercomparisons typically in the 3–5% range. The data define two very clear features. One is a trough of low heat-flow values, which runs continuously for 650 km along the northern edge of the lake, with values ranging between 0.46 and 0.98 heat-flow units (HFU) (19.2–41.0 mW/m^2). This feature correlates with surface exposure of Keweenawan mafic volcanics; it is believed to delineate a major crustal separation associated with the Midcontinent Rift and is filled to crustal thicknesses with mafic intrusives and extrusives. This feature has not been imaged with the seismic reflection profiling of GLIMPCE. The other heat-flow feature is an arcuate ridge of high heat-flow values (1.0–1.45 HFU; 41.8–60.7 mW/m^2), parallel to and south of the heat-flow trough. The highest areas of this ridge correspond to areas of thick rift-filling Keweenawan sediments. The high heat flow is modulated to lower values in areas where the thick sediments overlie highly thinned crust now containing large thicknesses of mafic volcanic rock. The heat-flow features show very good correlation with the magnetic anomaly map of Lake Superior, but only spotty correlation with the Bouguer gravity anomaly features.

Durant les étés de 1966 et de 1967 nous avons effectué au lac Supérieur 162 déterminations de flux thermique en utilisant les techniques océanographiques de mesure. Les résultats obtenus sont d'excellentes qualités, les comparaisons entre les données fournissent des précisions de l'ordre de 3 à 5%. Les résultats définissent deux structures nettement distinctes. Une représente un fossé caractérisé par de faibles valeurs de flux thermique, en continuité sur une distance de 650 km le long de la rive septentrionale du lac, et dont les valeurs varient de 0,46 à 0,98 unités de flux thermique (UFT) (19,2 à 41,0 mW/m^2). Ce fossé est corrélé avec l'exposition en surface des volcanites mafiques du Keweenawien, il est considéré comme marquant une séparation crustale majeure associée au rift Midcontinent, et ce fossé est rempli de roches mafiques intrusives et extrusives d'épaisseurs crustales. Cette structure n'apparaît pas dans les images du profil de sismique réflexion des levés GLIMPCE. L'autre structure est une crête arquée, caractérisée par des valeurs élevées de flux thermique (1,0 à 1,45 UFT; 41,8 à 60,7 mW/m^2), orientée parallèle et localisée au sud du fossé défini par les faibles valeurs de flux thermique. Les secteurs les plus hauts de cette crête correspondent aux régions du rift comblées de puissantes couches de sédiments keweenawiens. Le flux thermique élevé est modulé en valeurs plus faibles dans les régions où les épaisses accumulations de sédiments recouvrent une croûte considérablement amincie, contenant actuellement d'épaisses couches de roches volcaniques mafiques. Les zones de flux thermique présentent une excellent corrélation avec la carte des anomalies magnétiques du lac Supérieur, mais seulement une corrélation de nature ponctuelle avec les particularités qui se dégagent des anomalies gravimétriques de Bouguer.

[Traduit par la rédaction]

Can. J. Earth Sci. **31**, 698–708 (1994)

Introduction

In the past decade, enormous advances have been made in our understanding of the Proterozoic Midcontinent Rift System of North America. Lake Superior, which occupies the apex of this arcuate rift system, has been the focus of much of this effort through large coordinated programs such as the Great Lakes International Multidisciplinary Program on Crustal Evolution (GLIMPCE; Behrendt et al. 1989). There is now high-resolution gravity and magnetic coverage for this region (Hinze et al. 1982; Teskey et al. 1991), as well as numerous deep seismic reflection profiles (Cannon et al. 1989; Behrendt et al. 1990). In addition, the bedrock topography under Lake Superior has been characterized (Wold et al. 1982), the general crustal structure is known (Halls 1982; Tréhu et al. 1991; Hutchinson et al. 1992), and the bedrock geology surrounding the lake is well delineated (Cannon and Davidson 1982).

In the early 1960's, the Carnegie Institution of Washington initiated a program of heat-flow measurements in Lake Superior using oceanographic techniques (Hart and Steinhart 1965). During the summers of 1966 and 1967, 162 heat-flow measurements were made with a ~10 to 20 km grid spacing. A brief summary of the results was reported in Hart et al. (1968) and Steinhart et al. (1969), but the data were never interpreted nor published with full documentation. Not only does this study represent, next to Lake Baikal, the most detailed heat-flow survey in any continental area, the techniques utilized are still comparable with present state of the art. While surface heat flow cannot be inverted to give unique depth distributions of rock type or radioactivity, the detailed regional coverage of our data can help constrain the nature of the upper crustal geology under the lake when used in concert with existing gravity, magnetic, and seismic data.

[1]Lithoprobe Publication 581; Woods Hole Oceanographic Institution Contribution 8311.

Printed in Canada / Imprimé au Canada

Measurement techniques and data analysis

Thermal gradients

The basic heat-flow instrument was a 7 m piston corer (deployed from the United States Coast Guard cutter *Woodrush*), with five thermistors attached to outrigger fins (as originally developed for oceanic work by Gerard et al. 1962). The outrigger fins were designed to hold the thermistors 6.5 cm out from the core barrel, with a 4.2 cm projection ahead of the fin. The time constant of this arrangement brought temperatures to within 0.001°C of equilibrium in 4 min. The thermistors were routed, through a pressure-cased stepping-switch mounted on the corer, to the surface through conductors contained within the winch cable. A sensor in the pressure case was used to verify that all penetrations were within 5° of vertical. Typically, the corer was held just off bottom for 20 min to allow cooling to ambient water temperatures; resistance readings were taken a number of times during the 5–10 min period after probe insertion.

The thermistors, nominally ~5000 Ω at 4°C, were initially calibrated in the laboratory in a laminar-flow constant-temperature bath controlled over several minute time scales to 2×10^{-4}°C using a quartz-oscillator thermometer. This thermometer was in turn calibrated against the ice point of water, the triple point of phenoxybenzene, and other thermometers traceable to the National Bureau of Standards. Field calibrations were carried out after every 4–6 drops by intercomparing the five thermistors against a standard reference thermistor, all contained in an ice bath. Our typical thermistors showed a field drift rate of 1×10^{-3} to 2×10^{-3}°C/month, with occasional small episodic shifts of up to 5×10^{-3}°C. Damaged thermistors, or those showing larger shifts in calibration, were replaced immediately. Our calibration protocol allowed us to measure differential temperatures between thermistors to a level of 1×10^{-3} to 2×10^{-3}°C; with typical thermal gradients in the lake sediments of ~0.03 to 0.05°C/m, the precision of measuring thermal gradients was thus 2–5%.

Thermal conductivities

Thermal conductivities of the cored sediments were measured every 10–100 cm, using both a needle probe method (Von Herzen and Maxwell 1959) and by measuring the water contents of 10 cm "minicores" (by wet and dry weighing). Numerous tests involving intercomparisons of these two methods (Steinhart et al. 1969), measurements of gel standards, and many sediment replicates suggest a precision of 2–4% for our thermal conductivities. All values were corrected to in-situ temperatures. The site location data, measured temperatures, and thermal conductivities are available from the Depository of Unpublished Data.[2] Locations were determined by optical triangulation, radar fixes, and dead reckoning; in the worst cases, uncertainties in positioning could reach ±2–3 km. Figure A1 in the appendix gives a map of site locations.

Bottom-water temperature corrections

Unlike the oceans (Bullard et al. 1956), lake bottoms are not constant temperature environments on yearly time scales, and thermal gradients in the lake bottom sediments will be perturbed by any variation in bottom-water temperature. Fortunately, the bottom-water temperature of deep lakes is buffered, to first order, at the temperature of maximum density of water (~3.9°C at the surface, ~3.5°C at 200 m depth). The bottom-water temperature is typically maintained close to this maximum density temperature, independent of the mean annual air temperature (Steinhart and Hart 1965) and the amplitude of annual air-temperature variations is reduced typically by several orders of magnitude. Nevertheless, our goal was to determine heat flow to precisions of <5% and this necessitates making a correction for bottom-water temperature variations. To provide this information, we moored a temperature recorder in 200 m of water (47°18′N, 89°20′W) for the period from November 1, 1965 to October 10, 1966. The resulting temperature cycle shows a maximum temperature variation of only 1.2°C with a virtually constant 3.8°C temperature during summer stratification (July–November) and full lake mixing at ~3.2°C (March–May) after the winter turnover (see Fig. 32 in Hart et al. 1968). Ideally, it would be desirable to have bottom-water records for a variety of locations and for a period of years preceding the gradient measurements (Wang et al. 1986). We in fact attempted a variety of land-tethered, buoy-tethered and pop-up recorder placements, but only one was ever recovered.

The measured thermal gradients were corrected for this annual temperature cycle using a simple layer-over-a-half space model (Lachenbruch 1959) and the first 20 terms of the Fourier series representation of the annual cycle. The upper layer thickness was chosen to be in the range 0.5–2.0 m, depending on the shape of the thermal conductivity versus depth curve. We observed that this correction adequately linearized many of the gradients, but under- or overcorrected other gradients. Some locations in water shallower than 250 m tended to be undercorrected, and many locations, especially those deeper than 300 m, tended to be overcorrected. We assume this is because the amplitude of the annual bottom water temperature cycle is not constant everywhere in the lake but is a function of water depth; therefore we arbitrarily scaled the amplitude to empirically linearize the shallow gradients. Clearly, the phase of the annual cycle may also be a function of water depth, but consideration of bottom-water temperatures measured at each site prior to probe insertion suggests any phase uncertainty is masked by the amplitude effect. Several multiyear bottom-water temperature studies in other lakes have shown remarkable constancy of phase from year to year and location to location, but with significant amplitude variations (Lindqvist 1984; Allis and Garland 1976). This was not true for the Swiss lakes studied by Finckh (1981), but these lakes apparently never got cool enough to establish bottom water at <4°C. In addition, the air temperature variations at locations around Lake Superior were very similar in phase for the 5 years preceding our experiments; for example, at Marquette, Michigan, the annual air temperature cycles vary in phase by less than 2 weeks from year to year (United States Department of Commerce Local Climatological Data). In any event, the annual correction to the deepest (5–7 m) parts of the gradients, which we used to calculate the heat-flow values, is quite small (5–10%), so this first-order linearization scheme was felt to be completely adequate . Table 1 gives the calculated heat-flow values for the various depth intervals, using the amplitude-scaled annual temperature correction. These values are plotted and contoured in Fig. 1.

Longer term bottom-water temperature variations will also introduce perturbations into the sediment thermal gradients.

[2]The complete set of tabular data may be purchased from The Depository of Unpublished Data, Document Delivery, CISTI, National Research Council Canada, Ottawa, ON K1A 0S2, Canada.

TABLE 1. Corrected heat flow, Lake Superior

Site No.	Water depth	Probe depth	Linearized heat flow A	B	C	D	AM	Final heat flow	Site No.	Water depth	Probe depth	Linearized heat flow A	B	C	D	AM	Final heat flow
11	204	6.60	0.62	0.52	0.60	0.67	0.8	0.62±0.05	83	198	6.45	0.90	0.92	0.93	0.82	0.5	0.88±0.06
12	250	6.40	1.03	1.04	1.01	1.09	0.5	1.04±0.05	84	213	6.85	1.04	1.06	1.06	0.97	0.1	1.02±0.05
13	244	6.20	1.20	1.47	1.23	1.20	0.7	1.18±0.12	85	347	6.80	1.10	1.13	1.12	1.06	−0.1	1.11±0.04
15	229	6.08	0.99	0.97	0.96	1.01	0.8	0.97±0.10	86	238	6.80	1.17	1.17	1.18	1.15	0.1	1.16±0.04
16	259	6.67	1.07	1.08	1.07	1.11	0.4	1.09±0.04	87	204	6.50	0.97	0.99	0.99	0.92	0.4	0.97±0.05
17	274	6.96	1.11	1.12	1.11	1.13	0.2	1.15±0.04	89	201	6.80	1.11	1.10	1.12	1.09	0.4	1.10±0.03
19	256	6.80	1.03	1.04	1.01	1.06	0.3	1.06±0.05	91	247	6.80	1.11	1.08	1.11	1.08	0.1	1.10±0.04
20	223	4.47	1.05	1.03	1.03	1.06	0.7	1.06±0.10	92	256	6.60	0.98	0.98	1.00	0.93	0.3	0.98±0.05
21	229	5.27	0.80	0.73	0.79	0.88	1.0	0.85±0.15	93	229	6.70	1.00	0.96	1.00	0.98	0.3	0.98±0.04
22	259	6.82	1.14	1.14	1.14	1.19	0.3	1.15±0.05	94	256	6.85	1.06	0.98	1.05	1.05	0.1	1.05±0.04
23	265	6.50	1.12	1.13	1.11	1.17	0.5	1.13±0.04	95	229	6.90	0.59	0.53	0.58	0.55	0.8	0.56±0.04
24	289	4.50	1.08	0.92	0.97	1.08	0.8	1.00±0.15	96	165	4.80	1.42	1.67	1.08	0.87	0.8	0.92±0.15
25	247	6.88	1.08	1.13	1.08	1.10	0.4	1.09±0.04	97	177	6.50	0.75	0.70	0.75	0.72	0.6	0.73±0.03
26	256	6.85	0.54	0.55	0.54	0.60	0.4	0.56±0.05	98	210	6.90	1.00	0.97	1.00	0.98	0.3	0.99±0.04
27	183	6.85	0.75	0.82	0.78	0.86	1.0	0.82±0.05	99	238	6.75	1.08	1.01	1.07	1.07	0.3	1.07±0.04
28	311	6.85	0.43	0.46	0.43	0.50	0.6	0.48±0.05	100	244	6.10	1.08	0.96	1.05	1.06	0.8	1.05±0.05
29	177	6.82	0.61	0.60	0.60	0.69	1.6	0.61±0.05	101	201	4.90	1.84	1.95	1.40	1.22	0.4	1.10±0.18
30	177	6.85	0.65	0.69	0.65	0.73	0.8	0.67±0.05	102	250	6.95	0.58	0.50	0.57	0.59	0.8	0.58±0.04
31	189	6.42	0.65	0.62	0.62	0.72	1.0	0.65±0.05	103	177	6.85	0.93	0.91	0.93	0.93	1.7	0.92±0.03
32	165	6.00	0.82	0.75	0.78	0.87	1.6	0.86±0.05	104	181	6.40	0.84	0.69	0.72	0.79	2.4	0.92±0.05
33	174	6.62	0.77	0.74	0.75	0.83	1.2	0.77±0.05	105	208	6.50	0.97	0.86	0.91	0.95	1.9	0.97±0.05
34	177	6.10	0.81	0.72	0.79	0.87	1.5	0.82±0.05	106	247	6.70	1.33	1.31	1.31	1.33	0.8	1.33±0.04
37	174	6.50	0.81	0.71	0.79	0.87	1.2	0.82±0.05	108	268	6.30	1.17	1.19	1.21	1.18	0.8	1.18±0.03
38	192	6.70	0.80	0.75	0.79	0.84	0.8	0.82±0.04	109	223	6.60	0.93	0.91	0.93	0.93	1.6	0.92±0.03
39	210	6.70	0.86	0.87	0.83	0.90	0.7	0.88±0.04	110	238	6.70	1.18	1.15	1.16	1.18	2.0	1.15±0.04
40	190	5.05	0.99	0.98	0.95	1.03	0.8	0.96±0.07	111	229	6.80	1.11	1.08	1.10	1.11	1.2	1.10±0.03
41	192	6.60	0.99	0.98	0.97	1.03	0.8	0.99±0.05	114	296	6.85	1.13	1.09	1.09	1.13	0.7	1.11±0.03
42	227	6.60	0.77	0.68	0.78	0.80	0.2	0.79±0.04	115	192	6.30	1.22	1.12	1.15	1.20	1.2	1.18±0.05
43	219	6.60	0.74	0.65	0.75	0.75	0.2	0.76±0.04	116	205	5.30	0.97	0.95	0.95	0.97	1.2	1.01±0.06
44	232	6.60	1.06	0.96	1.06	1.06	−0.2	1.08±0.05	117	250	6.80	1.46	1.39	1.42	1.46	1.0	1.45±0.06
45	219	4.50	1.24	1.38	1.31	1.23	1.0	1.25±0.15	118	198	6.85	1.50	1.39	1.44	1.49	0.8	1.45±0.06
47	201	6.40	0.93	0.85	0.91	0.98	0.3	0.97±0.05	119	256	5.30	1.13	1.06	0.95	1.04	1.6	1.05±0.15
48	305	6.60	0.97	0.91	0.96	1.01	0.0	1.00±0.05	120	259	6.60	0.82	0.77	0.81	0.83	2.2	0.79±0.04
49	236	6.60	0.98	0.98	1.00	0.91	0.0	1.00±0.04	121	241	6.60	1.07	1.01	1.05	1.07	2.9	1.02±0.05
51	241	6.20	0.80	0.78	0.80	0.81	0.3	0.79±0.04	122	238	6.30	0.85	0.87	0.98	0.90	2.0	0.94±0.06
52	256	6.34	1.28	1.21	1.28	1.25	0.2	1.27±0.05	123	219	6.90	1.13	1.09	1.10	1.12	1.4	1.10±0.03
54	274	6.30	0.96	0.94	0.96	0.96	0.2	0.95±0.04	125	165	6.10	1.35	0.90	1.03	1.21	2.4	1.16±0.20
56	366	6.20	1.19	1.26	1.19	1.21	0.0	1.19±0.05	127	229	6.90	1.12	1.10	1.11	1.11	1.7	1.11±0.05
57	335	6.60	1.22	1.21	1.21	1.24	0.0	1.21±0.03	128	229	6.85	1.04	1.01	1.01	1.03	1.2	1.01±0.05
58	264	4.80	1.54	0.67	0.77	0.86	0.8	0.78±0.12	129	247	6.80	1.04	1.01	1.00	1.04	1.4	1.02±0.05
59	241	6.46	0.87	0.85	0.86	0.91	0.3	0.87±0.05	130	216	6.30	1.35	1.31	1.29	1.33	1.5	1.33±0.08
60	259	6.50	1.00	0.98	0.99	1.04	0.2	0.99±0.05	131	219	6.60	1.01	0.98	0.97	1.00	1.2	1.00±0.05
61	235	6.20	0.95	0.91	0.92	0.97	0.3	0.92±0.05	132	265	6.70	1.05	1.00	1.00	1.04	1.4	1.02±0.05
63	183	6.70	0.75	0.65	0.73	0.75	1.1	0.73±0.04	134	238	6.50	1.10	1.11	1.12	1.11	2.8	1.10±0.05
64	192	6.70	0.69	0.59	0.67	0.70	1.1	0.67±0.04	135	247	6.00	1.38	1.29	1.28	1.34	2.3	1.30±0.15
65	168	6.30	0.82	0.68	0.78	0.84	2.0	0.82±0.06	137	302	6.60	0.87	0.85	0.85	0.87	1.2	0.86±0.04
66	177	6.20	0.79	0.62	0.74	0.81	1.7	0.78±0.10	138	320	6.30	0.81	0.79	0.79	0.80	1.2	0.80±0.04
67	162	6.10	0.86	0.78	0.84	0.87	1.5	0.86±0.05	139	302	6.80	1.25	1.29	1.31	1.26	1.7	1.29±0.15
68	180	6.20	0.71	0.68	0.71	0.69	1.1	0.70±0.03	140	238	6.80	0.93	0.87	0.87	0.92	1.4	0.90±0.05
69	206	6.40	1.13	1.12	1.14	1.10	0.6	1.11±0.04	141	302	6.80	1.17	1.08	1.10	1.16	0.7	1.12±0.06
70	206	6.60	1.11	1.11	1.12	1.09	0.6	1.11±0.03	142	210	6.60	1.71	1.70	1.62	1.67	1.5	1.65±0.20
71	213	6.75	1.13	1.14	1.14	1.08	0.4	1.12±0.04	143	238	6.85	1.10	1.06	1.04	1.08	1.1	1.07±0.05
72	256	6.80	1.13	1.16	1.14	1.09	0.3	1.13±0.04	144	183	6.40	0.49	0.37	0.33	0.42	1.7	0.45±0.10
73	219	6.80	1.08	1.09	1.09	1.04	0.5	1.08±0.04	145	247	6.70	0.75	0.61	0.62	0.71	0.8	0.70±0.08
74	177	5.85	0.96	0.93	0.97	0.91	1.0	0.95±0.04	146	210	6.60	1.06	1.03	1.04	1.06	1.9	1.06±0.06
75	195	6.10	0.48	0.36	0.46	0.45	1.4	0.46±0.05	147	210	6.00	1.18	1.49	1.35	1.23	3.3	1.28±0.15
76	183	6.30	0.62	0.57	0.62	0.59	1.1	0.60±0.04	148	223	6.40	1.17	1.16	1.15	1.17	1.2	1.15±0.04
77	192	5.80	0.79	0.80	0.82	0.77	0.8	0.79±0.03	149	247	6.00	1.17	1.17	1.18	1.17	1.2	1.17±0.04
78	192	6.90	0.72	0.73	0.72	0.71	0.4	0.72±0.03	150	311	6.80	1.09	1.11	1.10	1.09	0.7	1.10±0.03
79	204	6.70	0.71	0.72	0.71	0.71	0.5	0.71±0.03	152	192	6.80	1.00	0.99	1.01	1.00	1.9	1.00±0.05
80	192	6.80	1.06	1.08	1.08	1.00	0.3	1.06±0.04	153	320	6.90	1.10	1.08	1.11	1.10	0.4	1.09±0.04
81	201	6.50	0.99	1.01	1.01	0.95	0.6	0.99±0.05	154	210	6.90	1.03	0.99	1.06	1.05	1.2	1.04±0.04
82	201	6.20	0.92	0.92	0.94	0.86	0.6	0.89±0.05	155	229	6.20	1.29	1.21	1.29	1.29	1.7	1.29±0.10

TABLE 1 (*concluded*)

Site No.	Water depth	Probe depth	Linearized heat flow A	B	C	D	AM	Final heat flow	Site No.	Water depth	Probe depth	Linearized heat flow A	B	C	D	AM	Final heat flow
156	293	6.20	1.32	1.24	1.32	1.31	1.0	1.28±0.06	177	238	6.50	0.86	0.88	0.88	0.87	1.4	0.88±0.05
157	247	6.90	1.03	1.03	1.08	1.05	1.2	1.04±0.05	178	265	6.10	1.16	1.00	0.97	1.08	0.8	1.00±0.08
158	216	6.90	1.05	1.01	1.07	1.06	1.2	1.05±0.04	179	192	6.10	1.46	1.42	1.44	1.45	1.9	1.45±0.10
159	183	6.90	0.72	0.72	0.74	0.73	1.0	0.72±0.04	180	256	6.70	0.91	0.82	0.83	0.87	1.0	0.86±0.04
160	183	6.85	1.13	1.13	1.15	1.14	1.6	1.13±0.04	181	253	6.40	1.00	0.92	0.98	1.00	1.1	0.98±0.04
162	247	6.90	0.74	0.70	0.73	0.74	0.8	0.73±0.04	182	219	6.00	1.37	1.25	1.25	1.33	2.0	1.30±0.10
163	219	6.70	0.95	0.87	0.92	0.94	1.2	0.94±0.04	183	210	6.90	1.16	1.11	1.12	1.15	1.7	1.14±0.05
164	219	6.80	1.00	1.00	1.00	1.00	1.4	1.01±0.04	184	219	6.85	0.93	0.88	0.90	0.93	1.6	0.92±0.04
165	265	6.80	0.91	0.91	0.91	0.92	1.0	0.92±0.04	185	219	6.85	1.21	1.14	1.17	1.20	1.4	1.19±0.05
166	223	6.10	1.07	1.01	1.03	1.05	1.4	1.05±0.04	186	265	6.80	1.15	1.08	1.09	1.13	0.8	1.12±0.04
167	247	6.70	1.10	1.07	1.08	1.09	0.8	1.09±0.04	188	366	6.00	1.38	1.34	1.36	1.38	1.2	1.36±0.06
168	283	6.30	1.17	1.23	1.17	1.17	1.1	1.17±0.06	189	238	6.05	1.35	1.38	1.41	1.38	2.5	1.40±0.20
169	232	6.80	0.82	0.81	0.84	0.83	1.1	0.83±0.03	192	210	6.85	0.75	0.72	0.73	0.75	1.0	0.73±0.03
171	201	6.45	0.99	0.92	0.93	0.97	1.6	0.97±0.05	193	265	6.50	1.29	1.26	1.29	1.29	0.8	1.28±0.04
173	210	5.60	0.99	0.88	0.92	0.96	1.6	0.96±0.10	194	241	6.40	1.15	1.13	1.16	1.16	0.8	1.14±0.04
174	229	6.80	0.91	0.77	0.75	0.84	2.5	0.85±0.10	195	229	4.70	1.59	0.54	0.65	0.74	1.7	0.73±0.10
175	192	6.00	1.13	0.79	0.84	1.00	2.7	1.00±0.15	196	238	6.90	0.86	0.87	0.88	0.87	1.2	0.87±0.03
176	192	6.60	0.94	0.88	0.90	0.93	3.0	0.93±0.04	197	210	6.90	0.96	0.94	0.96	0.97	1.1	0.96±0.04

NOTES: Site locations are plotted on Fig. A1 in the appendix. Water depth and probe penetration depths are in meters; the latter was determined by the "mud line" on the core barrel or core body assembly. A, B, C, and D correspond to depth intervals over which heat flow was calculated. For 1966 stations (11-102), these correspond to the intervals between thermistors 1−3, 2−4, 3−5, and 4−5, respectively. For 1967 stations (103-197) these correspond to intervals between thermistors 1−2, 2−4, 3−4, and 3−5, respectively. AM, the amplitude multiplier, is the factor by which the annual bottom-water temperature cycle was multiplied to achieve the best linearity over all intervals. The final heat-flow value is based on the deepest two intervals; the value and the assigned error is subjectively weighted according to depth of penetration, overall linearity of all intervals, size of the annual cycle correction, and variability of the measured conductivities. Heat-flow values are given in 10^{-6} cal/(cm^2 · s); to convert to mW/m^2, multiply by 41.84.

The maximum coupling will occur for decadal time scales, with longer period changes (>1000 years) producing shifts in the gradients without introducing measurable nonlinearity into the gradients. As long as the climate stays within the bounds where the bottom water can be buffered at the maximum density point (−7° to 8°C mean annual air temperature), these long-term variations will affect the absolute heat-flow values only slightly, and the relative values for different locations in a given lake should be quite insensitive to such climatic effects.

Topographic and sedimentation effects

Much of Lake Superior is underlain by relatively smooth bedrock topography covered by 50−75 m of Pleistocene sediment (Wold et al. 1982). Rougher topography is encountered in the eastern section of the lake which is marked by a series of north−south-trending valleys filled with 75−175 m of sediment. And the northwest shore is paralleled by a major valley structure filled with up to 275 m of sediment. For the typical valley and ridge topography of the eastern lake, model calculations (see Von Herzen and Uyeda 1963) suggest that heat-flow values in valleys may be enhanced by 3−5% due to the geometric effect, and reduced by 2−4% due to refraction effects related to the sediment fill. There may also be a 5−8% reduction due to the deposition of the sedimentary fill during the last glacial period (Hutchison 1985). Owing to the partial offsetting nature of these effects, we expect that the measured heat-flow values will not show significant (>5−10%) effects due to these topographic and sedimentation effects. We have also tested this conclusion empirically by comparing measured heat-flow values on adjacent ridges and valleys in the southeast part of the lake (Fig. 1) where the regional heat-flow variations are small. We see no evidence for topographic−sedimentation effects at even the 5% level.

The situation with the major bedrock valley running along the northwest shore of the lake is not so benign, however, and it is obvious from Fig. 1 that several major heat-flow lows (values as low at 0.5 heat-flow units (HFU; 1 HFU = 41.84 mW/m^2)) are present in this region, which may be related to the thick sedimentation in this valley. The shallowest sediment in this valley appears to have a similar stratigraphy to surface lake sediments elsewhere in the lake, with some 4 m of postglacial gray clay underlain by 10−15 m of varved red and gray glacial clays. The unusual sediment thickness is created by a few hundred meters of underlying mixed glacial tills and clays. If we assume these were deposited rapidly some 15 000 − 20 000 years ago, modeling shows that the thermal gradient will be lower than steady state by approximately 20% (Von Herzen and Uyeda 1963); values will be 28% low for valleys with 275 m of sedimentation. The thickest sediment is observed in the valley section between 91.0−91.5°W, and heat-flow station 28 is directly in this valley; the observed heat-flow value of 0.48 HFU would thus correct up to a value of 0.66. This is still a very low heat-flow value, suggesting that the heat-flow lows along this shore are real and not just a sedimentation effect. Empirical support for this comes from a careful correlation of measured heat flow and sediment thickness (Wold et al. 1982) in this region. In locations just outside the bedrock valley region, with normal 50−60 m sediment thicknesses, heat flows of 0.61−0.65 are noted (sites 11, 29, 31). These are similar to the site 28 corrected value. Furthermore, the northeastern end of this long valley, where it runs between Isle Royale and the mainland (88.8−89.5°W), consistently has 200−225 m of sediments in it, but apparently transects a sharp heat-flow boundary at about 89.3°W where heat flow increases (going northeast) from values of 0.5−0.6 HFU to a plateau of values around 1.0−1.05 HFU. Clearly here the low values may be too low by 0.1−0.2 HFU

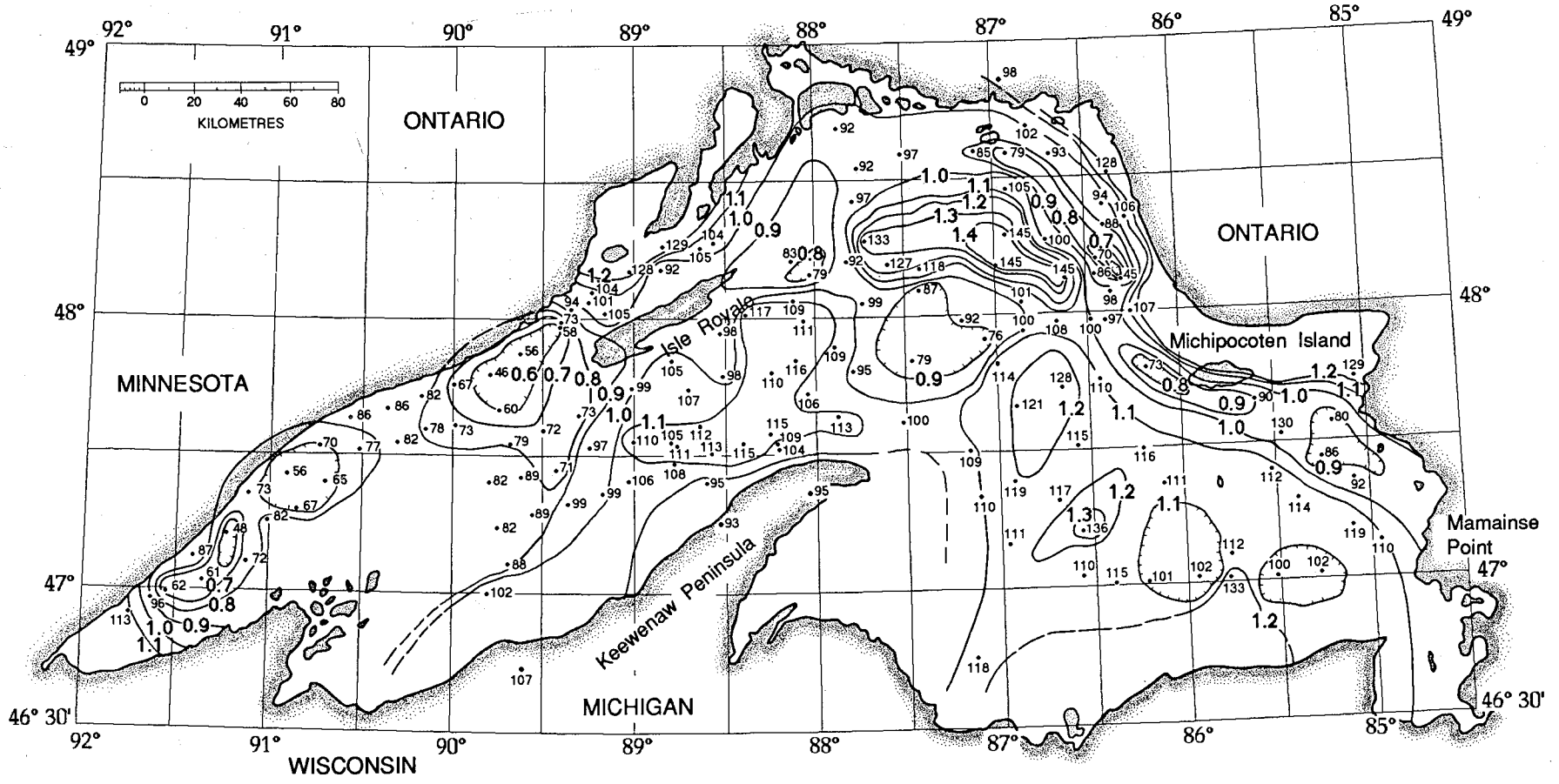

FIG. 1. Heat-flow contour map of Lake Superior. Values are taken from Table 1 and given as heat-flow units (HFU) × 100; values with errors larger than ±0.15 HFU are not plotted. Plotted values can be converted to mW/m^2 by multiplying by the factor 0.4184. Hatched areas represent local minima. Contouring was done manually, taking into account the formal errors assigned to each point. This map adapted, corrected, and updated from Steinhart et al. (1969). The four onshore heat-flow values are from Roy (1963) and Jessop and Lewis (1978).

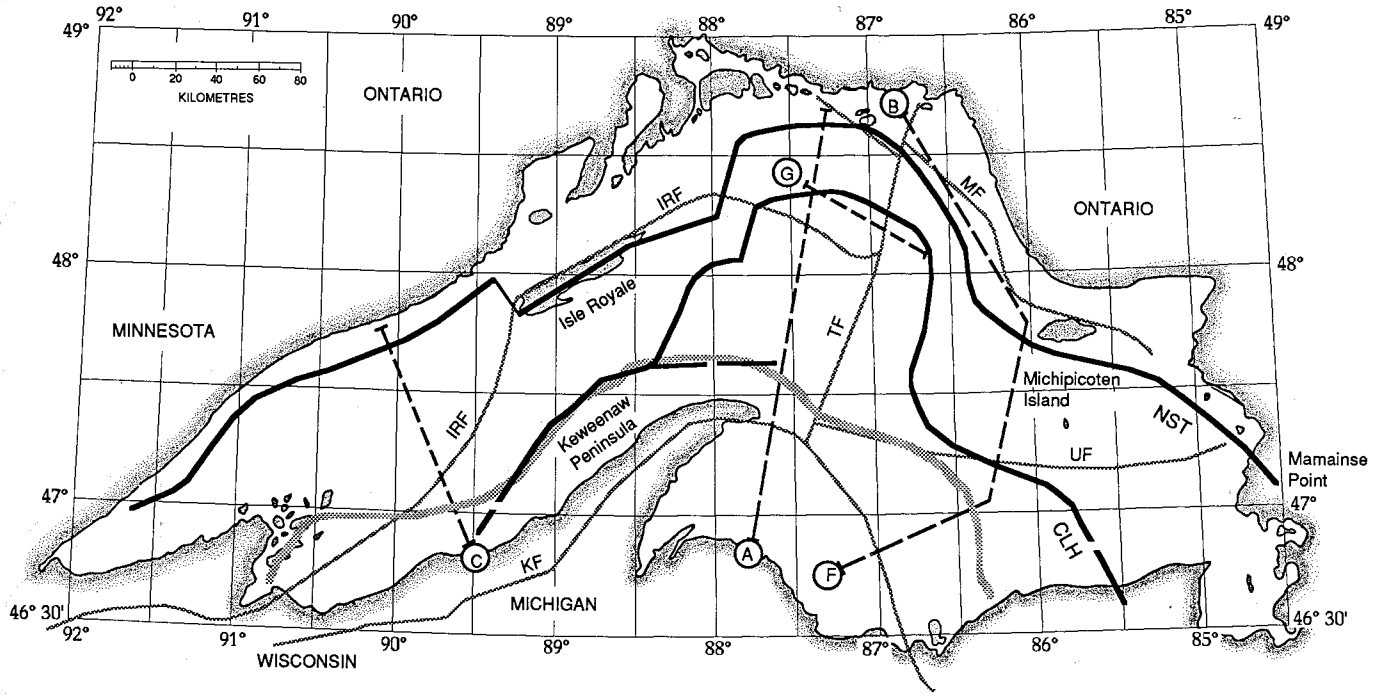

FIG. 2. Map of Lake Superior showing trends of north-shore heat-flow trough (NST) and central lake heat flow high (CLH) as heavy solid lines. Also shown are locations of various inferred faults (thin patterned lines) from Hinze et al. (1982), the GLIMPCE seismic reflection track lines (heavy broken lines) from Cannon et al. (1989), and the axis of thickest rift-filling sediment (thick patterned lines) from McGinnis (1990). IRF, Isle Royal fault; KF, Keweenaw fault; MF, Michipicoten fault; TF, Thiel fault; UF, unnamed fault.

owing to sedimentation effects, but the general existence of an elongate heat flow low (0.6−0.8 HFU) along this shore of the lake, terminated at the southwest end of Isle Royale by more normal values (>0.9 HFU), is quite a real feature.

Similarly, in the northeast part of the lake, there is an elongate heat-flow low running parallel to the shore of the lake with values as low as 0.45 HFU. This heat-flow trough trends across the grain of the sediment-filled bedrock valleys in this region, and there is no correlation between heat flow and bedrock topography, again showing that these features are real and not simply artifacts of topography and sedimentation.

Precision

We assess precision in two ways. First, three measurements were made in close proximity (<1.8 km) at sites 69, 70, and 100. The values of 1.11 ± 0.04, 1.11 ± 0.03 and 1.05 ± 0.05 HFU agree within stated precision. Secondly, intercomparison of the general consistency of values in areas where the heat flow is smoothly varying over large distances suggests individual measurements are precise at stated error limits (typically 3−5%). Consider, for example, the broad area of normal heat flow just north of the Keweenaw peninsula, with 22 values in the range 1.05−1.16 HFU. Only one measurement in this broad contiguous area has a value outside this range (0.85 ± 0.15, site 21), and this site has a large error due to short penetration and larger resulting annual cycle correction.

Accuracy is a much more difficult problem to assess, in particular because of the longer term temperature fluctuations related to glacial−interglacial periods. As noted earlier, we are more interested in inter-site consistency of values, and this aspect will be largely independent of long-term climatic effects. However, some indication of accuracy can be obtained by comparison of our lake measurements with four onland bore hole values reported by Roy (1963) and Jessop and Lewis (1978); these are shown in Fig. 1 (two on the Keweenaw Peninsula, one adjacent to the south shore, west of the Keweenaw Peninsula, and one close to the north shore at 87°). In all four cases, the onland values fit within the pattern of adjacent lake values very closely, certainly to within 10−15%.

Results and discussion

The observed heat flow in Lake Superior shows an unusually large range, from 0.46−1.45 HFU (considering only values determined to 10% or better). The features defined by this variation (Fig. 1) are fairly regular, with a crescent-shaped heat-flow low or trough extending virtually continuously for 650 km along the northern shore of the lake from 91.5°W to 85.0°W. Except for the westernmost part of this north shore trough (NST), higher and more normal heat flow values occur between the NST and the actual shore of the lake, emphasizing that this is a trough and not just the southern edge of a low heat flow province.

The NST is paralleled on the south for much of its extent by a broad heat-flow ridge or series of highs, starting northwest of the Keweenaw Peninsula and extending in an arcuate belt around through the eastern end of the lake, broadening as it goes east. We designate this as the central lake high (CLH). There is an isolated low lying off the northeast end of the Keweenaw Peninsula, which defines the high in this region as a ridge, not an extended plateau of high values. There is a suggestion of a right lateral offset in the NST at ~89.3°W and of a left lateral offset in both the NST and the CLH at 87.8°W. This latter feature could also just be a kink in both the NST and CLH, as there are only limited heat flow stations to the northwest of this area.

Figure 2 is a schematic figure showing the trend lines of the

NST and CLH, as well as some of the structural discontinuities inferred from other studies. The locations of four GLIMPCE seismic reflection profiles are also shown, along with the trend line of the thickest rift sedimentation. First, with respect to the various inferred faults, there are some aspects of the heat-flow data that support several of these structures. The Isle Royale fault (IRF) coincides with the NST from Isle Royale east to 88°W; to the west, however, this fault diverges away from the NST, essentially paralleling the 1.0 HFU contour. Along the northeast shore, the Michipicoten fault (MF), and its northwest extension, follows the NST rather well for its whole extent from 85.5 to 87.5°W. On the other hand, the structure (UF) running due east from the tip of the Keweenaw Peninsula has no obvious expression in the heat-flow data. No heat-flow data were obtained in the regions of the Keweenaw fault (KF), as a result of our inability to penetrate the sediments with the corer. The Thiel fault (TF) does cross well-constrained heat-flow territory, however, and has no obvious expression. In fact, it crosses both the NST and the highest part of the CLH at almost right angles, with no perturbation of these features. We did note above a possible offsetting north–south fault structure at 87.8°W, but this is well separated from the location inferred for the Thiel fault.

In comparing the heat flow map with the gravity and magnetic maps (Hinz et al. 1982) of Lake Superior, there is a superficial similarity in all three due to the general arcuate appearance of all three maps. The NST coincides for almost its whole length with a sharp magnetic high, and the broad magnetic low which characterizes most of the central axis of the lake (Teskey et al. 1991) corresponds quite well with the ridge (CLH) of normal to high heat-flow values shown in Fig. 2. In general, we would argue that the magnetic highs track Keweenawan mafic volcanic rocks, which are also loci for low heat-flow values.

In comparison with the gravity field (Hinze et al. 1982), the NST follows a gravity high from the easternmost part of the lake to about 86.5°W, at which point the gravity high loops south while the NST loops north; both join again at about 88°W and track each other across to the west end of Isle Royale. Here the gravity high drops to the south shore of the lake and delimits a major bull's eye, with no corresponding feature at all in the heat flow. The NST continues along the northwest shore of the lake and aligns with a new gravity high starting at about 90.5°W. While there are a number of low gravity areas in the lake, most are localized and do not correspond very well with the arcuate heat-flow ridge (CLH).

There is at least a mild expectation that heat flow and gravity fields should covary, as the heat generation of igneous and orthogneissic rocks shows a good inverse correlation with rock density (Steinhart et al. 1969; Rybach and Buntebarth 1982; Pollack 1982). Dense mafic rocks have typically only 10–30% the heat generation of granitic rocks; ultramafic (mantle)rocks will have the highest density, but as little as 0.1–1% the heat generation of a granite. The general lack of correspondence between the heat flow and gravity fields of Lake Superior can probably be attributed to the presence of a significant sediment section along the rift axis; while uniformly low in density, sediments may be either high or low in heat generation depending on their particular mineralogical makeup. This will lead to a decoupling of heat flow and gravity, but may also provide a potential way to distinguish different sedimentary sections which may not be otherwise distinctive in gravity or seismic properties.

We come now to the question of what the heat flow variation in Lake Superior actually means in terms of crustal lithologies. Earlier we noted our opinion that the NST heat-flow low corresponds to the presence of mafic volcanic rock and requires the relative absence of either felsic rocks or sediments with significant radioactivity. This is borne out by consideration of the geology of the lake shore: Keweenawan mafic igneous rocks are abundant along the northwest shore between 89.5 and 92°W; volcanic rocks then occur on Isle Royale, the islands along the far north shore, and again on Michipicoten Island and Mamainse Point. In fact, the boundary marking the shoreward limit of volcanic rock outcrop in and along the lake (Green 1982; Hinze et al. 1982) corresponds extremely well with the 1.0–1.1 HFU contour that marks the northern boundary of the NST.

In attempting to reconcile this strong correspondence between low heat flow and Keweenawan mafic volcanics and the results of the seismic reflection profiles located in Fig. 2, we encounter difficulty. In Fig. 3, we compare our heat flow data along three of these seismic reflection profiles (C, A, and B–F). Where lines C, A, B, and F cross the NST, there are only minimal thicknesses of volcanic rocks shown in the seismic sections, and in fact most of the crustal thickness in sections A and C is shown as normal prerift Archean to Late Proterozoic crust, without significant thinning related to the rifting (Samson and West 1992; Cannon et al. 1989; Green et al. 1989). The northern part of the Lake Superior rift was formed in the Archean Shebandowan granite–greenstone terrain (Klasner et al. 1982; Van Schmus and Hinze 1985). Heat-flow values in typical granite–greenstone terrains of the Superior Province average 0.9–1.0 HFU (Jessop and Lewis 1978; Drury 1987; Sclater et al. 1980). How can the NST be marked by heat-flow values in the 0.6–0.8 HFU range if it is underlain by only thin Keweenawan volcanics on top of a normal crustal thickness of Archean granite–greenstone lithologies? We would argue that in fact the Keweenawan volcanic–plutonic section must be enormously thicker than shown on the seismic reflection cross sections and that any significant upper crustal Archean section must be virtually absent. Replacing 15 km of typical Archean upper crust (with heat generation of 1.5–1.6 $\mu W/m^3$) by 15 km of gabbro–basalt (with heat generation of 0.6–0.7 $\mu W/m^3$) will lower the heat flow by about 0.3–0.4 HFU; this is about the minimum required to provide the lowest values in the NST (for conversion, note that a heat generation value of 1 $\mu W/m^3$ will produce a heat flow of 0.024 HFU/km of rock column). Modeling of large aperture seismic data along profile A by Tréhu et al. (1991) shows a possible ridge of high velocity lower crustal material intruding into midcrustal levels at about the point where the NST crosses profile A. Because of the inverse relationship between density and heat production, every drop in heat flow of 0.1 HFU should be accompanied by an increase in Bouguer anomaly of about 20–25 mGal (1 Gal = 1 cm/s^2). The NST is not generally marked by +100 mGal gravity anomalies, so additional offsetting features are required to minimize the gravity anomaly.

Explanation for the CLH is more problematic. Figure 2 shows the axis of thickest sedimentation in the rift structure (McGinnis 1990), and this coincides in part with the CLH (western and eastern arms). However, the northward bulge of the CLH departs significantly from the sedimentary basin axis; line A crosses this peak on the CLH (Fig. 3), and line G runs almost along it, and both lines show the presence of a small

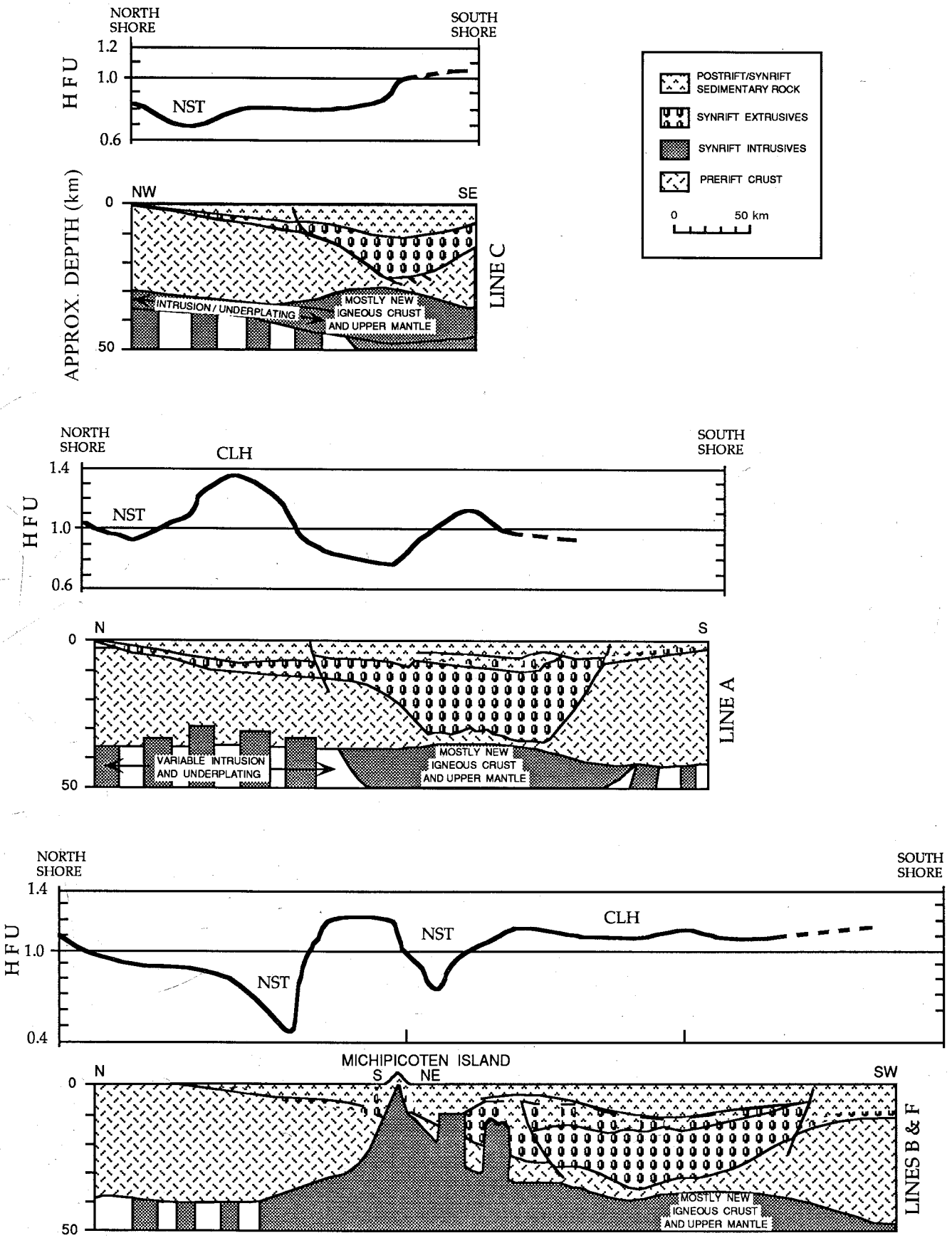

FIG. 3. Comparison of heat-flow profiles (in heat-flow units, HFU) with GLIMPCE seismic reflection lines A, B, C, and F (adapted from Hutchinson et al. 1992). Locations of seismic profiles are shown on Fig. 2; heat-flow profiles are based on the contouring in Fig. 1. Interleaved patterns indicate regions containing mixed units.

subsidiary sedimentary basin formed by a half-graben bordered on the south by the Isle Royale fault. While the sedimentary thickness in this basin is less than that along the main axis of the central basin, the key difference is that the sediment sequence in the main basin overlies a massive thickness (20–30 km) of what is interpreted as mafic volcanics (i.e., preexisting crust is highly thinned here). The subsidiary sediment basin along profile G is interpreted as having only a thin underlying volcanic sequence on top of a more or less normal thickness of preexisting crust. The sediments in this basin presumably need to be much higher in heat production than typical Archean shield because the heat flow along this part of the CLH is 1.3–1.45 HFU; this is significantly higher than average Archean shield values (0.9–1.0 HFU). The heat generation of average Superior Province surface crust is about 1.5 $\mu W/m^3$ (Jessop and Lewis 1978; Shaw et al. 1976; Fahrig and Eade 1968). Even relatively high heat generation sediments such as shales have typical heat generation values of only 2.0 $\mu W/m^3$ (Taylor and McClennan 1985; Condie 1993), so the differential between prerift upper crust and such a sediment is small $\sim$0.5 $\mu W/m^3$. This only leads to a heat-flow anomaly of 0.12 HFU for 10 km of sediments; either the prerift heat flow in this area was unusually high to begin with or the sediments must be extraordinarily high in radioactivity.

Along the rest of the CLH, the heat flow represents a balance between high values associated with thick rift-basin sediments and lower values associated with thinned crust and increased thickness of underlying mafic volcanics. The axis of thickest sedimentation and the axis of greatest crustal thinning do not coincide, in general, due to the asymmetry of the half-graben style of tectonism (Cannon et al. 1989). Along profile A, the axis of thickest sedimentation lies well south of the axis of thinnest crust; the broad heat-flow low just northeast of the Keweenaw Peninsula coincides with the axis of maximum crustal thinning. Along profile C, the sedimentary trough axis lies north of the axis of maximum crustal thinning; we would suggest that the area just north of the Keweenaw peninsula, where the CLH crests to values of 1.15 HFU, represents an area where the sedimentary basin axis is well offset from the crustal thinning axis (or perhaps where the crustal thinning is less extensive).

Summary

The heat flow in Lake Superior is a function of three components (ignoring the small fraction that originates sub-Moho). One is the normal Archean–Proterozoic prerift crust with thicknesses of $\sim$40 km and heat flow of 0.90–1.0 HFU. The second is Keweenawan mafic volcanics and intrusives, with low heat production leading to heat flows of 0.15–0.20 HFU per 10 km of thickness. The third is the Keweenawan basin-filling sediments, with high heat production leading to heat flows of perhaps 0.4–0.5 HFU per 10 km of thickness. The ultimate heat flow at any point in the rift will depend on how much of the prerift crust has been thinned and replaced with Keweenawan mafic rocks and how much of this consequent lowering in heat flow is then compensated for by the higher heat production of the rift-basin sediments.

The major feature of the Lake Superior heat-flow map is the trough of low heat flow (NST) paralleling the northern edge of the lake. The lowest points on this NST require the absence of most of the pre-rift crust, and, at most, a thin layer of basin sediments. In other words, the crust has been extended and filled with Keweenawan mafic rocks. Klasner et al. (1982) argue for as much as 50 km of north–south separation or extension across the Midcontinent Rift in the Lake Superior region (see their Fig. 13). Based on the width of the NST, we would argue that at least 20–25 km of crustal separation has occurred, with almost complete filling of this rift with mafic igneous rocks. Being largely intrusive, these may not maintain a coherent layering and so will appear confused on the reflection profiles. The crustal section we envision might look like that on profile B–F, (Fig. 3) at Michipicoten Island (from Hutchinson et al. 1992). This model faces an obvious difficulty with respect to the gravity signature expected for such a mafic crustal section and the spotty degree to which the NST correlates with high gravity. To accommodate this problem, we would argue that perhaps the crust is locally thicker (underplated?) in the actual region of the NST, with this greater thickness not resolvable in refraction profiles (Epili and Mereu 1989) or the more regional crustal thickness maps of Halls (1982).

The other pronounced feature in the Lake Superior heat-flow map is the arcuate ridge of high heat flow that occupies the center of the lake, paralleling the NST. The high heat flow along this ridge is controlled by the thickness of rift-basin sediments, and offset by thinned crust with a high mafic igneous rift-filling component.

It will obviously be useful to test and extend this schematic model by a more detailed comparison of the seismic, gravity, magnetic and heat-flow data sets.

Acknowledgments

This work was made possible through the creative willingness of the United States Coast Guard and, in particular, the outstanding help and professionalism of the officers and crew of the U.S.C.G.C. *Woodrush* (the key names have been lost in the mists of time!). The work was done while all three authors were staff members at the Department of Terrestrial Magnetism (DTM), Carnegie Institution of Washington. The late Merle Tuve encouraged us to try yet one more thing that wasn't terrestrial magnetism. The machine shop and electronic shop personnel at DTM were instrumental in designing and building most of the instrumentation. S.R.H. thanks Woods Hole Oceanographic Institution for supporting him to finally write up this microoceanography project. Very constructive reviews were provided by R. Von Herzen , T. Lewis, and D. Issler.

Allis, R.G., and Garland G.D. 1976. Geothermal measurements in five small lakes of northwest Ontario. Canadian Journal of Earth Sciences, **13**: 987–992.

Behrendt, J.C., Green, A.G., Lee, M.W., Hutchinson, D.R., Cannon, W.F., Milkereit, B., Agena, W.F., and Spencer, C. 1989. Crustal extension in the Midcontinent Rift System—results from GLIMPCE deep seismic reflection profiles over Lakes Superior and Michigan. *In* Properties and processes of earth's lower crust. *Edited by* R.F. Mereu, S. Mueller, and D.M. Fountain. American Geophysical Union, Geophysical Monograph 51, pp. 81–89.

Behrendt, J.C., Hutchinson, D.R., Lee, M., Thornber, C.R., Trehu, A., Cannon, W., and Green, A. 1990. GLIMPCE seismic reflection evidence of deep-crustal and upper-mantle intrusions and magmatic underplating associated with the Midcontinent Rift system of North America. Tectonophysics, **173**: 595–615.

Bullard, E.C., Maxwell, A.E., and Revelle, R. 1956. Heat flow through the deep sea floor. Advances in Geophysics, **3**: 153–181.

Cannon, W.F., and Davidson, D.M., Jr. 1982. Bedrock geologic map of the Lake Superior Region. *In* Geology and Tectonics of the Lake Superior Basin. *Edited by* R.J. Wold and W.J. Hinze. Geological Society of America, Memoir 156, pp. 5–14.

Cannon, W.F., Green, A.G., Hutchinson, D.R., Lee, M., Milkereit, B., Behrendt, J.C., Halls, H.C., Green, J.C., Dickas, A.B., Morey, G.B., Sutcliffe, R., Spencer, C. 1989. The North American Midcontinent Rift Beneath Lake Superior from GLIMPCE seismic reflection profiling. Tectonics, **8**: 305–332.

Condie, K.C. 1993. Chemical composition and evolution of the upper continental crust: Contrasting results from surface samples and shales. Chemical Geology, **104**: 1–37.

Drury, M. 1987. Heat flow provinces reconsidered. Physics of the Earth and Planetary Interiors, **49**: 78–96.

Epili, D., and Mereu, R.F. 1989. The GLIMPCE seismic experiment: onshore refraction and wide-angle reflection observations from a fan line over the Lake Superior Midcontinent Rift System. *In* Properties and processes of Earth's lower crust. *Edited by* R.F. Mereu, S. Mueller, and D.M. Fountain. American Geophysical Union, Geophysical Monograph 51, pp. 93–101.

Fahrig, W.F., and Eade, K.E. 1968. The chemical evolution of the Canadian Shield. Canadian Journal of Earth Sciences, **5**: 1247–1252.

Finckh, P. 1981. Heat flow measurements in 17 perialpine lakes. Geological Society of America Bulletin, Part II, **92**: 452–514.

Gerard, R., Langseth, M.G., and Ewing, M. 1962. Thermal gradient measurements in the water and bottom sediment of the western Atlantic. Journal of Geophysical Research, **67**: 785–803.

Green, A.G., Cannon, W.F., Milkereit, B., Davidson, A., Behrendt, J.C., Spencer, C., Hutchinson, D.R., Lee, M.W., Agena, W.F., and Morel-a-l'Huisser, P. 1989. A "GLIMPCE" of the deep crust beneath the Great Lakes. *In* Properties and processes of Earth's lower crust. *Edited by* R.F. Mereu, S. Mueller, and D.M. Fountain. American Geophysical Union, Geophysical Monograph 51, pp. 65–80.

Green, J.C. 1982. Geology of Keweenawan extrusive rocks. *In* Geology and tectonics of the Lake Superior Basin. *Edited by* R.J. Wold and W.J. Hinze. Geological Society of America, Memoir 156, pp. 47–55.

Halls, H.C. 1982. Crustal thickness in the Lake Superior region. *In* Geology and tectonics of the Lake Superior Basin. *Edited by* R.J. Wold and W.J. Hinze. Geological Society of America, Memoir 156, pp. 239–243.

Hart, S.R., and Steinhart, J.S. 1965. Terrestrial heat flow: measurement in lake bottoms. Science (Washington, D.C.), **149**: 1499–1501.

Hart, S.R., Steinhart, J.S., and Smith, T.J. 1968. Heat flow. Carnegie Institution of Washington Year Book, **66**: 52–57.

Hinze, W.J., Wold, R.J., and O'Hara, N.W. 1982. Gravity and magnetic anomaly studies of Lake Superior. *In* Geology and tectonics of the Lake Superior Basin. *Edited by* R.J. Wold and W.J. Hinze. Geological Society of America, Memoir 156, pp. 203–221.

Hutchinson, D.R., Lee, M.W., Behrendt, J., Cannon, W.F., and Green, A.G. 1992. Variations in the reflectivity of the Moho transition zone beneath the Midcontinent Rift System of North America: results from true-amplitude analysis of GLIMPCE data. Journal of Geophysical Research, B, **97**: 4721–4737.

Hutchison, I. 1985. Effects of sedimentation and compaction on oceanic heat flow. Geophysical Journal of the Royal Astronomical Society, **82**: 439–459.

Jessop, A.M., and Lewis, T. 1978. Heat flow and heat generation in the Superior Province of the Canadian Shield, Tectonophysics, **50**: 55–77.

Klasner, J.S., Cannon, W. F., and Van Schmus, W.R. 1982. The pre-Keweenawan tectonic history of southern Canadian Shield and its influence on formation of the Midcontinent Rift. *In* Geology and tectonics of the Lake Superior Basin. *Edited by* R.J. Wold and W.J. Hinze. Geological Society of America, Memoir 156, pp. 27–46.

Lachenbruch, A.H. 1959. Periodic heat flow in a stratified medium, with application to permafrost problems. United States Geological Survey Bulletin, 1083(A).

Lindqvist, J.G. 1984. Heat flow density measurements in the sediments of three lakes in northern Sweden. Tectonophysics, **103**: 121–140.

McGinnis, L.D. 1990. Lake Superior rift basins. Eos, **71**: 995.

Pollack, H.N. 1982. The heat flow from the continents. Annual Review of Earth and Planetary Sciences, **10**: 459–481.

Roy, R.F. 1963. Heat flow measurements in the United States. Ph.D. thesis, Harvard University.

Rybach, L., and Buntebarth, G. 1982. Relationships between the petrophysical properties density, seismic velocity, heat generation, and mineralogical constitution. Earth and Planetary Science Letters, **57**: 367–376.

Samson, C., and West, G.F. 1992. Crustal structure of the Midcontinent rift system in eastern Lake Superior from controlled-amplitude analysis of GLIMPCE deep reflection seismic data. Canadian Journal of Earth Sciences, **29**: 636–649.

Sclater, J.G., Jaupart, C., and Galson, D. 1980. The heat flow through oceanic and continental crust and the heat loss of the Earth. Reviews of Geophysics and Space Physics, **18**: 269–311.

Shaw, D.M., Dostal, J., and Keays, R.R. 1976. Additional estimates of continental surface Precambrian shield composition in Canada. Geochimica et Cosmochimica Acta, **40**: 73–83.

Steinhart, J.S., and Hart, S.R. 1965. Heat flow. Carnegie Institution of Washington Year Book, **64**: 296–300.

Steinhart, J.S., Hart, S.R., and Smith, T.J. 1969. Heat flow. Carnegie Institution of Washington Year Book, **67**: 360– 367.

Taylor, S.R., and McClennan, S.M. 1985. The continental crust: its composition and evolution. Blackwell Scientific Publications, Oxford.

Teskey, D.J., Thomas, M.D., Gibb, R.A., Dods, S.D., Kucks, R.P., Chandler, V.W., Fadaie, K., and Phillips, J.D. 1991. High resolution aeromagnetic survey of Lake Superior, Eos, **72**: 81–86.

Tréhu, A., Morel-à-l'Huissier, P., Meyer, R., Hajnal, Z., Karl, J., and Mereu, R. 1991. Imaging the Midcontinent Rift Beneath Lake Superior Using Large Aperture Seismic Data. Geophysical Research Letters, **18**: 625–628.

Van Schmus, W.R., and Hinze, W.J. 1985. The Midcontinent Rift System. Annual Review of Earth and Planetary Sciences, **13**: 345–383.

Von Herzen, R., and Maxwell, A.E. 1959. The measurement of thermal conductivity of deep-sea sediments by the needle-probe method. Journal of Geophysical Research, **64**: 1557–1563.

Von Herzen, R., and Uyeda, S., 1963. Heat flow through the eastern Pacific ocean floor. Journal of Geophysical Research, **68**: 4219–4250.

Wang, K., Shen, P.Y., and Beck, A.E. 1986. The effects of thermal properties structure and water bottom temperature variation on temperature gradients in lake sediments. Canadian Journal of Earth Sciences, **23**: 1257–1264.

Wold, R.J., Hutchinson, D.R., and Johnson, T.C. 1982. Topography and surficial structure of Lake Superior bedrock as based on seismic reflection profiles. *In* Geology and tectonics of the Lake Superior Basin. *Edited by* R.J. Wold and W.J. Hinze. Geological Society of America, Memoir 156, pp. 257–272.

Appendix

Figure A1 gives a map of the site locations for the Lake Superior heat-flow project.

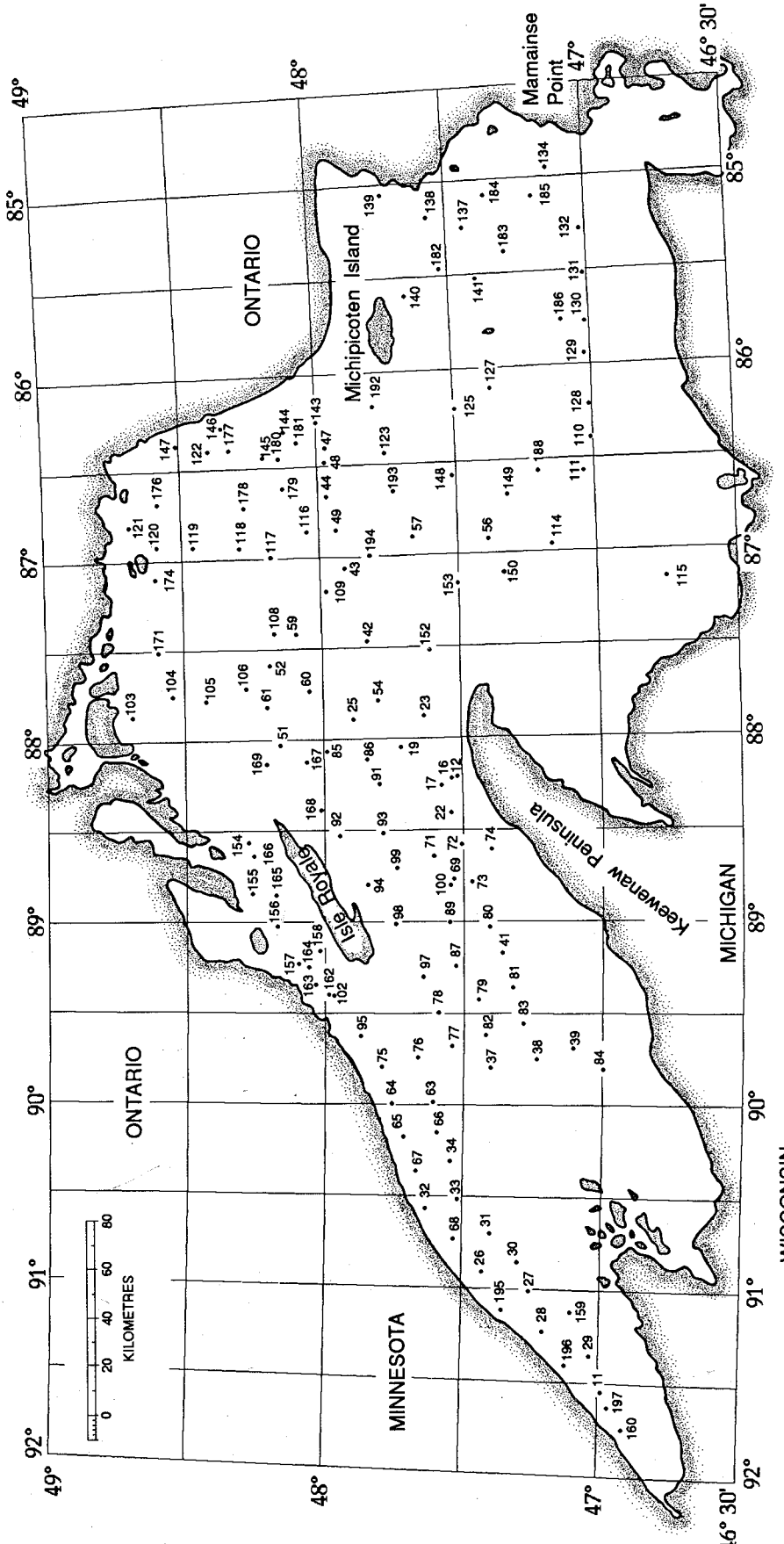

FIG. A1: Site location map, Lake Superior heat-flow project. Location data is from Table A1, Depository of Unpublished Data[2]; only sites with successful heat-flow measurements are shown.